Revealing the heterogeneous nucleation and growth behaviour of grains in inoculated aluminium alloys during solidification

Yijiang Xu[1], Daniele Casari[2], Ragnvald H. Mathiesen[2], Yanjun Li[1*]

[1] Department of Materials Science and Engineering, Norwegian University of Science and Technology (NTNU), N-7491 Trondheim, Norway

[2] Department of Physics, Norwegian University of Science and Technology (NTNU), N-7491 Trondheim, Norway

*Corresponding author: E-mail address: yanjun.li@ntnu.no

Abstract

An in-situ X-ray radiographic study on the grain nucleation and grain growth of inoculated Al-10Cu and Al-20Cu alloys during isothermal melt solidification and directional solidification conditions with constant cooling rates has been carried out. The influence of addition level of inoculation particles, cooling rates, and temperature gradient on the nucleation rate and growth kinetics of grains have been quantitatively studied. The deterministic nature of the heterogeneous nucleation of aluminium grain on inoculant particles is revealed. Numerical microstructure models have been developed to simulate the nucleation and growth behavior of aluminum grains and a good agreement between the experimental results and simulation results has been achieved.

Keywords: Heterogeneous nucleation, Grain growth, Solidification, Aluminium alloy

1. Introduction

Grain refinement by inoculation is a common practice during the casting and solidification of Al and Al alloys. As summarized in several review papers [1-4], the grain refinement mechanisms have been much understood through extensive studies in the past decades.

Lots of experimental works have been made to study grain refinement behaviour in inoculated Al alloys, such as thermal analysis [5, 6], post-solidification characterization of cast samples, in-situ X-ray diffraction [7-9] and in-situ X-radiography study [10-13]. However, comprehensive in-situ studies on the heterogeneous nucleation and grain growth under dedicated solidification conditions are still needed to reach an in-depth understanding on the nucleation kinetics under different solidification conditions (cooling rate, temperature gradient) and different solute/grain refiner addition levels, the nucleation ceasing mechanisms, and the grain growth kinetics.

Besides, many numerical and analytical grain size prediction models have been developed [14-28] to better understand the nucleation and grain growth behaviour. However, most of the grain size prediction models [14, 16, 17, 24, 26, 29], are based on the assumption of spherical/globular grain growth kinetics. Thus, a more sophisticated model including globular to dendritic transition (GDT) and dendritic growth kinetics needs to be developed, by which the influence of grain morphology transition on the nucleation kinetics and predicted grain size can be quantitively investigated. Furthermore, most of the published models intended for directional solidification [20, 24-26], are still based on a local isothermal melt solidification assumption. Therefore, new models with a rigorous treatment of grain nucleation on inoculant particles under the temperature gradient effect during is still demanded.

In the present work, an integrated study by in-situ X-radiography and numerical modelling will be carried out to reveal the heterogeneous nucleation and growth behaviour of grains during solidification of inoculated Al alloys.

2. Experimental

The materials used in the experimental study are Al-10Cu and Al-20Cu (wt.%) alloys prepared by melting 5N (99.999 wt.%) purity aluminum and 4N (99.99 wt.%) purity copper in a clay graphite crucible using a Nabertherm melting furnace. After complete melting and mixing of the raw metals, different levels of commercial Al-5Ti-1B (wt.%) master alloy were added to the melt and finally cast into a copper mold. Thin plate samples with dimension of $5 \times 50 \times 0.2 \pm 0.01$ mm (X×Y×Z) are prepared from the cast ingots by cutting, grinding and polishing.

The microfocus X-radiography setup applied in the present study, including the XRMON Gradient Furnace, CCD camera and X-ray source with a Mo transmission target, has been described in detail in Ref. [30-32]. The sample was aligned in a configuration where the broad surface (X-Y plane) of the sheet-like sample is perpendicular to the gravity (Z || g), by which the melt convection and grain motion were greatly reduced. The Bridgman furnace was operated in the so-called near-isothermal mode [12, 28], and also in standard directional solidification mode with imposed temperature gradients G along the sample length direction (G || Y). Constant cooling rates $\dot{T}$, in the range of 0.025-1.0 K/s, were applied by a controlled power down technique at two heater elements located at two sides of the field of view (FOV) along the sample length direction (Y-direction). The images were recorded it-situ at a frame rate of 2 Hz.

3. Model

The numerical model used in this work is an extension to a previous grain size prediction model [26], now modified to include the dendritic growth and effect of temperature gradient on nucleation. The heterogeneous nucleation of grains on inoculant particles is based on the free growth criterion [17]. A particle size distribution is measured as input parameters. Fig.1 is a schematic drawing to show the nucleation of new grains around one single grain during isothermal melt solidification and directional solidification. The solute diffusion field and temperature gradient induced inhibited nucleation zone (INZ, the red region) are rigorous treated based on the local undercooling shown in Fig.1a1 and 1b1, and particles can only be active for nucleation in the active nucleation zone (ANZ, the green region).The detailed model description and mathematical equations could be found in Ref. [28, 33].

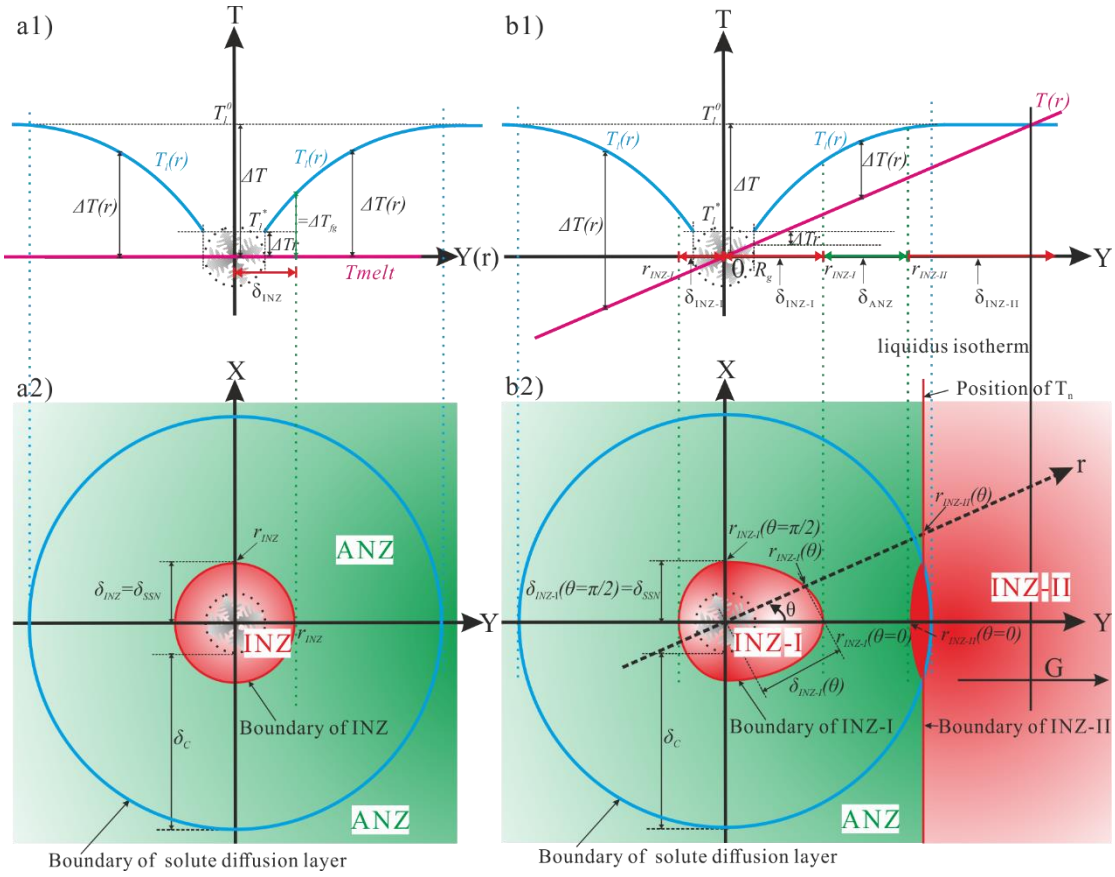

Fig. 1. Schematic drawing showing the nucleation of new grains around one single grain during (a) isothermal melt solidification and (b) directional solidification. (a1)(b1) Liquidus temperature $T_l(r)$, melt temperature $T(r)$ and the corresponding local undercooling of the liquid $\Delta T(r)$ outside the grain envelope that along the Y direction. (a2)(b2) 2-Dimensional illustration of the inhibited nucleation zone (INZ), active nucleation zone (ANZ), and the corresponding boundary.

4. Results and discussion

4.1 Isothermal melt solidification

The in-situ X-radiography image sequences during isotermal melt solidification of 0.05 wt.% Al-5Ti-1B inoculated Al-20Cu alloy at three constant cooling rates, 0.025, 0.1 and 0.5 K/s are shown in Fig. 2. Due to the difference in Cu concentration between the liquid and solid phases, the solid Al grains show a brighter contrast. The nucleation kinetics and growth of each individual grain could be tracked from the image sequences. Under all these cooling conditions, equiaxed grain structures were obtained. However, as the cooling rate increases, the total number of grains appearing in the FOV also increases.

The evolution of the total number of primary α-Al grains in the FOV as a function of undercooling below the nucleation temperature (since the first grain is observed) have been extracted and plotted in Fig. 3. Three stages nucleation kinetics can be observed. When the relative undercooling is small (⩽~1 K), the numbers of grains formed in the FOV under different cooling rates are nearly the same at the same undercooling values. This is because the volume fraction of solid grains is very low at small undercooling, and therefore the solute rejection from the growing grains has little effect on the nucleation, and the initiation of new grains only depends on the number of available potent inoculant particles. It is a strong evidence to support the athermal nucleation theory and free growth model [17], that the nucleation of grains is just a function of undercooling and independent of cooling rate at the beginning of solidification. However, at higher undercoolings, the number of grains in the FOV for different cooling rate is different and the nucleation rate is smaller in the low cooling rate cases. This means that the solute diffusion zone around growing grains, in terms of solute suppressed nucleation zone or inhibited nucleation zone, has played an important role in preventing the nucleation of new grains in the zones [20, 24]. In this stage, there is a competition between grain growth, solute segregation and external cooling. Once the real cooling rate is less than the reduction rate of liquidus temperatue of the remaing melt (casued by the enrichment of solute in the residual liquid metal) [26], the nucleation process stops and the number density reaches the maximum. That is stage three and all the space between the grains become nucleation-free zones. It can also be seen from Fig.2 that, the average distance between neighbour grains and the areas of nucleation-free zones decrease with inreasing cooling rate.

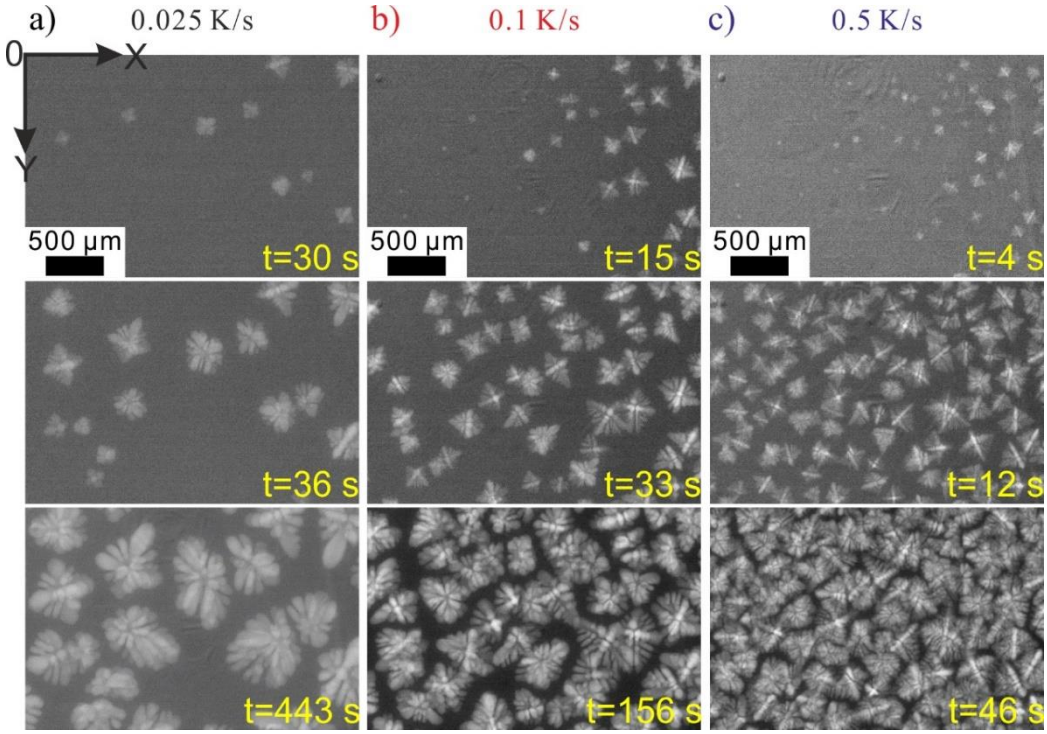

Fig. 2. Selected X-radiographic images from the in-situ isothermal melt solidification of 0.05 wt.% Al-5Ti-1B inoculated Al-20Cu alloy under three different cooling rates: (a) 0.025 K/s, (b) 0.1 K/s and (c) 0.5 K/s.

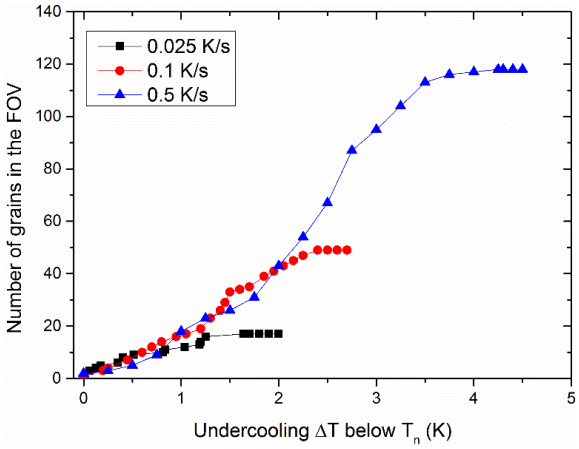

Fig. 3. The evolution of total number of grains in the FOV as a function of undercooling below nucleation temperature for the three different solidification cases shown in Fig.2.

Fig. 4a shows predicted grain size of Al-10Cu alloy solidified under 0.5 K/s cooling rate, as a function of addition level of refiner, in comparison to the experimentally determined grain sizes from in-situ X-radiography. As can be seen, the model prediction with considering the dendritic morphology transition based on hemispherical tip growth have a good agreement with the experimental results, showing the high sensitivity of the model to the grain refiner addition level. As addition level increases, grain size decreases. Fig. 4b shows experimental determined and predicted grain size as a function of cooling rate for 0.05 wt.% Al-5Ti-1B inoculated Al-10Cu alloy. As can be seen, the predicted grain sizes show quantitatively good agreement with the measured values. It confirms that the present model has a good prediction capability. Moreover, the solute segregation stifling mechanism and solute suppressed nucleation zone treatment proposed in the model is validated.

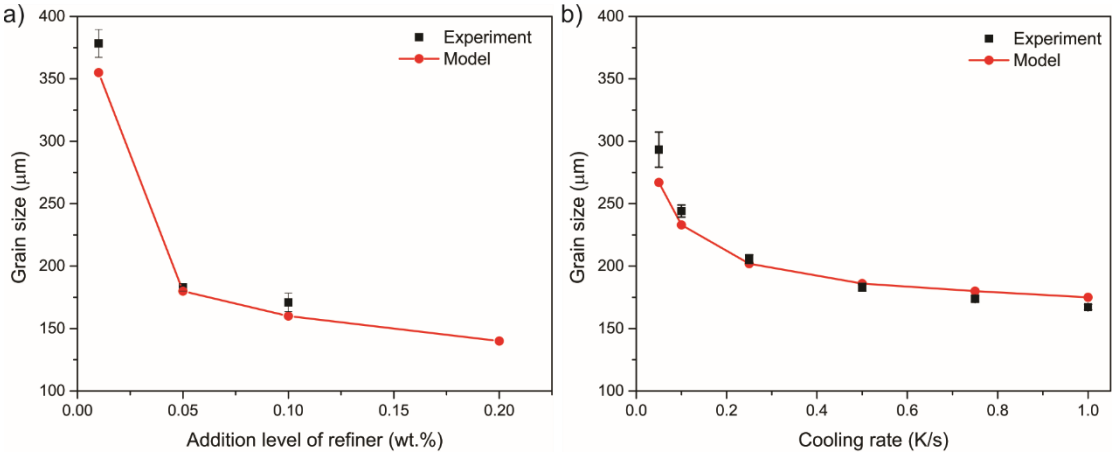

Fig. 4. (a) grain size of Al-10Cu alloy solidified under 0.5 K/s cooling rate, as a function of addition level of refiner. (b) grain size as a function of cooling rate for 0.05 wt.% Al-5Ti-1B inoculated Al-10Cu alloy.

4.2 Directional solidification

Fig. 5 shows the X-radiographic images recorded during solidification of 0.05 wt.% Al-5Ti-1B inoculated Al-20Cu alloy at a cooling rate of 0.1 K/s, with three different temperature gradients (G=0, 5, 10 K/mm) along the Y-direction. By comparing these threee conditions, we can find that for the higher G condition, the total number of grains is less and the grains become more elongated, and the length of different primary dendrite arms of each grain is very different. Besides, the grain nucleation front of the directional solidification cases, as labeled by the dashed lines in Fig. 5b and 5c, propagates gradually towards the hot side of the FOV. The new grains formed in the nucleation front have the influence of blocking the growth of previously formed grains behind them by solute diffusion field impingement. For those grains without new grains forming ahead of them, the grain growth is free to continue, and accordingly these grains will develop into elongated morphologies, e.g., Grain A and Grain B in Fig. 5c.

The corresponding evolution of total number of grains in the FOV as a function of solidification time is shown in Fig. 6. As can be seen, the number of grains in the FOV increases with the solidification time, i.e., decreasing melt temperature, until a maximum value is reached and then remains constant. During near-isothermal melt solidification, the evolution of grain number in the FOV is quite smooth. However the curves of directional solidification, especially at G = 10 K/mm, show a step-terrace character, indicating that the propagation of nucleation front has wave-like nature. This is consistent with the finding by Prasad et al.[13, 34]. In isothermal melt solidification, a maximum number of 49 equiaxed grains is achieved in the FOV within 24 s, corresponding to an average nucleation rate of 2.97 $mm^{-3}s^{-1}$. However, in directional solidification, it takes 94 s and 147.5 s to form only 30 and 18 grains in the whole FOV for G = 5 and G=10 K/mm cases, respectively. The corresponding average nucleation rate are 0.46 $mm^{-3}s^{-1}$ and 0.18 $mm^{-3}s^{-1}$, respectively, which are about one order of magnitude smaller than that in isothermal solidification at the same cooling rate. The results show that the nucleation rate and the final grain number is reduced significantly when a temperature gradient is applied, although the cooling rate during the solidification is the same.

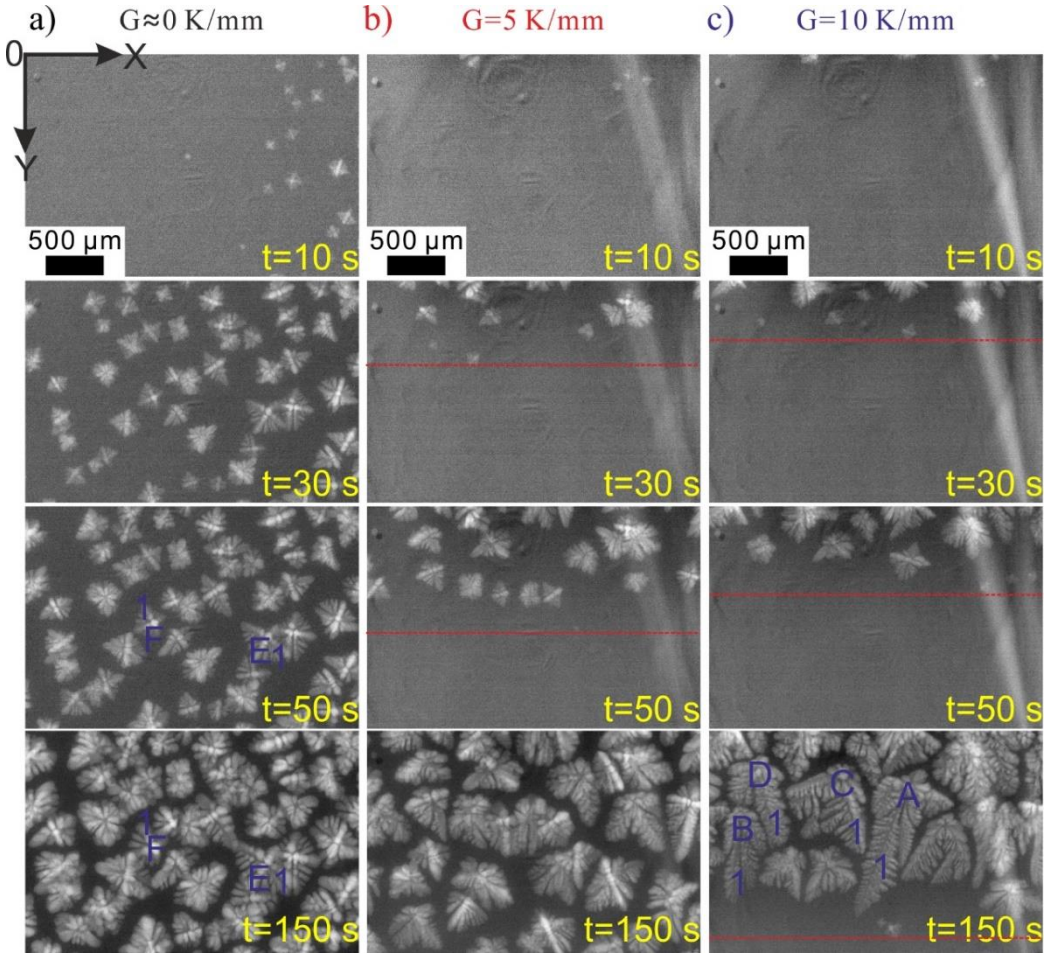

Fig. 5. Selected X-radiographic images from in-situ solidification of inoculated Al-20Cu alloy at 0.1 K/s cooling rate under three different temperature gradients G: (a) $G_Y \cong 0$, (b) G_Y=5 K/mm and (c) G_Y=10 K/mm.

The grain growth in G=0 and G = 10 K/mm at 0.1 K/s are also quantitively analyzed from the in-situ X-radiographic image sequences. Each dendrite arm is labeled with a number 1 for grains A ~ F, as illustrated in Fig. 5. The primary dendrite arm length is measured from the nucleation center of grains, and the results are plotted in Fig. 7. As can be seen, during isothermal melt solidification, e.g., Grain E and F, the growth of equiaxed grains stops earlier due to the soft impingement of solute diffusion field with that of neighbor surrounding grains. However, at G = 10 K/mm directional solidification, grain growth along the temperature gradient direction towards the hot side of the melt could last a longer time due to the delay or lack of nucleation of new grains in front of the dendrite tip owing to the temperature gradient effects. For grain A and B, the growth velocity is almost constant.

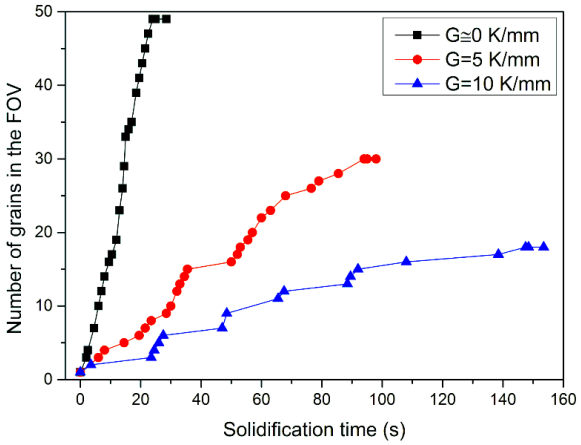

Fig. 6. Evolution of the total number of grains in the FOV as a function of solidification time in three solidification cases shown in Fig. 5.

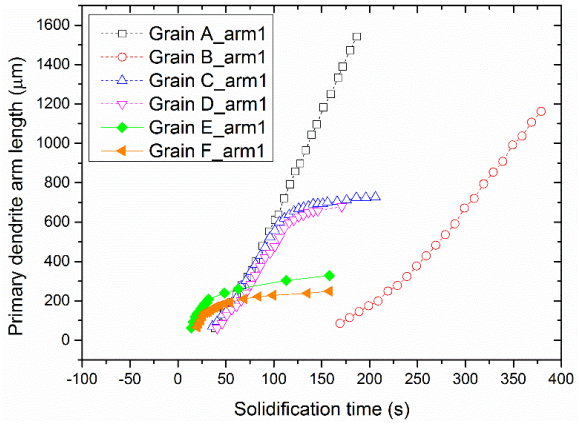

Fig. 7. Evolution of individual primary dendrite arm length over time for several grains selected from in-situ X-radiographic images (labeled in Fig. 5) in two solidification conditions: isothermal and directional solidification with G_Y=10 K/mm ($\dot{T} = 0.1\ K/s$).

Fig. 8 shows the predicted and measured grain number density as a function of temperature gradient for the inoculated Al-20Cu alloy solidified at 0.1 K/s. As can be seen, the model reproduces the experimentally determined evolution trend of grain number density in relation to the temperature gradient *G*. The good agreement between the model prediction and experimental results proves that the proposed modeling approach to treat the inhibited nucleation zone and active nucleation zone around growing equiaxed grains under temperature gradient effects is feasible.

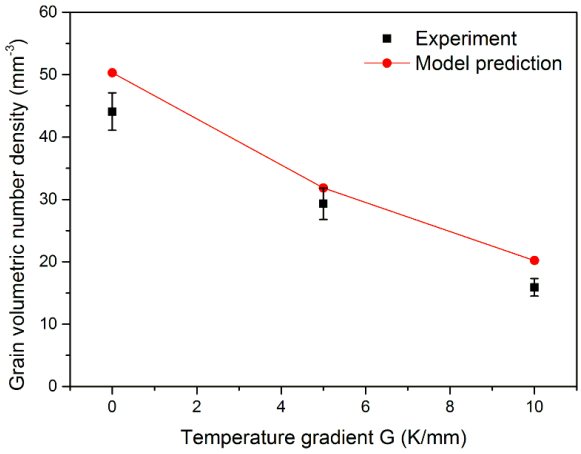

Fig. 8. Predicted and measured grain number density of the 0.05 wt.% Al-5Ti-1B inoculated Al-20Cu alloy as a function of temperature gradient for the same cooling rate of 0.1 K/s.

5. Conclusions

The kinetics of heterogeneous nucleation and grain growth in isothermal melt and directional solidification of Al-Ti-B inoculated Al-Cu alloys has been studied by in-situ X-radiography. The effect of cooling rate, addition level of grain refiner, and temperature gradient are quantitively investigated and revealed. Furthermore, a new grain size prediction model considering GDT and the effect of *G* on nucleation has been applied to simulate the grain nucleation and growth and a good agreement between the predicted results and experimental results are achieved. The free growth concept and the solute segregation stifling mechanism for grain nucleation have been verified by the in-situ experiments and numerical modelling.

Acknowledgements

The financial support by The Research Council of Norway and industrial partners, for the PRIMAL project (project number: 236675), is gratefully acknowledged.

References

[1] B.S. Murty, S.A. Kori, M. Chakraborty. Grain refinement of aluminium and its alloys by heterogeneous nucleation and alloying, International Materials Reviews 47 (2002) 3-29.
[2] T.E. Quested. Understanding mechanisms of grain refinement of aluminium alloys by inoculation, Materials Science and Technology 20 (2004) 1357-1369.
[3] M.A. Easton, M. Qian, A. Prasad, D.H. StJohn. Recent advances in grain refinement of light metals and alloys, Current Opinion in Solid State and Materials Science 20 (2016) 13-24.
[4] A.L. Greer. Overview: Application of heterogeneous nucleation in grain-refining of metals, The Journal of Chemical Physics 145 (2016) 211704.
[5] M. Johnsson, L. Backerud, G. Sigworth. Study of the mechanism of grain refinement of aluminum after additions of Ti- and B-containing master alloys, Metallurgical Transactions A 24 (1993) 481-491.
[6] M. Johnsson. Grain refinement of aluminium studied by use of a thermal analytical technique, Thermochimica Acta 256 (1995) 107-121.
[7] N. Iqbal, N.H. van Dijk, S.E. Offerman, M.P. Moret, L. Katgerman, G.J. Kearley. Real-time observation of grain nucleation and growth during solidification of aluminium alloys, Acta Materialia 53 (2005) 2875-2880.
[8] N. Iqbal, N.H. van Dijk, S.E. Offerman, N. Geerlofs, M.P. Moret, L. Katgerman, G.J. Kearley. In situ investigation of the crystallization kinetics and the mechanism of grain refinement in aluminum alloys, Mater. Sci. Eng. A 416 (2006) 18-32.
[9] N. Iqbal, N.H. van Dijk, S.E. Offerman, M.P. Moret, L. Katgerman, G.J. Kearley. Nucleation kinetics during the solidification of aluminum alloys, Journal of Non-Crystalline Solids 353 (2007) 3640-3643.
[10] G. Reinhart, N. Mangelinck-Noël, H. Nguyen-Thi, T. Schenk, J. Gastaldi, B. Billia, P. Pino, J. Härtwig, J. Baruchel. Investigation of columnar–equiaxed transition and equiaxed growth of aluminium based alloys by X-ray radiography, Mater. Sci. Eng. A 413–414 (2005) 384-388.
[11] H. Nguyen-Thi, G. Reinhart, N. Mangelinck-Noël, H. Jung, B. Billia, T. Schenk, J. Gastaldi, J. Härtwig, J. Baruchel. In-Situ and Real-Time Investigation of Columnar-to-Equiaxed Transition in Metallic Alloy, Metallurgical and Materials Transactions A 38 (2007) 1458-1464.
[12] A.G. Murphy, W.U. Mirihanage, D.J. Browne, R.H. Mathiesen. Equiaxed dendritic solidification and grain refiner potency characterised through in situ X-radiography, Acta Mater. 95 (2015) 83-89.
[13] A. Prasad, S.D. McDonald, H. Yasuda, K. Nogita, D.H. StJohn. A real-time synchrotron X-ray study of primary phase nucleation and formation in hypoeutectic Al–Si alloys, J. Cryst. Growth 430 (2015) 122-137.
[14] I. Maxwell, A. Hellawell. A simple model for grain refinement during solidification, Acta Metall. 23 (1975) 229-237.
[15] P. Thévoz, J.L. Desbiolles, M. Rappaz. Modeling of equiaxed microstructure formation in casting, Metall. Trans. A 20 (1989) 311-322.
[16] P. Desnain, Y. Fautrelle, J.L. Meyer, J.P. Riquet, F. Durand. Prediction of equiaxed grain density in multicomponent alloys, stirred electromagnetically, Acta Metall. 38 (1990) 1513-1523.
[17] A.L. Greer, A.M. Bunn, A. Tronche, P.V. Evans, D.J. Bristow. Modelling of inoculation of metallic melts: application to grain refinement of aluminium by Al–Ti–B, Acta Materialia 48 (2000) 2823-2835.

[18] M.A. Easton, D.H. StJohn. A model of grain refinement incorporating alloy constitution and potency of heterogeneous nucleant particles, Acta Materialia 49 (2001) 1867-1878.
[19] A.L. Greer, T.E. Quested, J.E. Spalding. Modelling of grain refinement in directional solidification. in: Schneider WA, (Ed.). Light Metals 2002. Minerals, Metals & Materials Soc, Warrendale, 2002. pp. 687-694.
[20] T.E. Quested, A.L. Greer. Grain refinement of Al alloys: Mechanisms determining as-cast grain size in directional solidification, Acta Materialia 53 (2005) 4643-4653.
[21] B. Böttger, J. Eiken, M. Apel. Phase-field simulation of microstructure formation in technical castings – A self-consistent homoenthalpic approach to the micro–macro problem, Journal of Computational Physics 228 (2009) 6784-6795.
[22] M. Qian, P. Cao, M.A. Easton, S.D. McDonald, D.H. StJohn. An analytical model for constitutional supercooling-driven grain formation and grain size prediction, Acta Materialia 58 (2010) 3262-3270.
[23] H. Men, Z. Fan. Effects of solute content on grain refinement in an isothermal melt, Acta Materialia 59 (2011) 2704-2712.
[24] D. Shu, B. Sun, J. Mi, P.S. Grant. A quantitative study of solute diffusion field effects on heterogeneous nucleation and the grain size of alloys, Acta Materialia 59 (2011) 2135-2144.
[25] D.H. StJohn, M. Qian, M.A. Easton, P. Cao. The Interdependence Theory: The relationship between grain formation and nucleant selection, Acta Materialia 59 (2011) 4907-4921.
[26] Q. Du, Y.J. Li. An extension of the Kampmann-Wagner numerical model towards as-cast grain size prediction of multicomponent aluminum alloys, Acta Materialia 71 (2014) 380-389.
[27] M. Martorano, D. Aguiar, J. Arango. Multigrain and Multiphase Mathematical Model for Equiaxed Solidification, Metall. Mater. Trans. A 46 (2015) 377-395.
[28] Y. Xu, D. Casari, Q. Du, R.H. Mathiesen, L. Arnberg, Y. Li. Heterogeneous nucleation and grain growth of inoculated aluminium alloys: An integrated study by in-situ X-radiography and numerical modelling, Acta Materialia 140 (2017) 224-239.
[29] T.E. Quested, A.L. Greer. The effect of the size distribution of inoculant particles on as-cast grain size in aluminium alloys, Acta Materialia 52 (2004) 3859-3868.
[30] A.G. Murphy, D.J. Browne, W.U. Mirihanage, R.H. Mathiesen. Combined in situ X-ray radiographic observations and post-solidification metallographic characterisation of eutectic transformations in Al–Cu alloy systems, Acta Materialia 61 (2013) 4559-4571.
[31] H. Nguyen-Thi, G. Reinhart, G. Salloum-Abou-Jaoude, D.J. Browne, A.G. Murphy, Y. Houltz, J. Li, D. Voss, A. Verga, R.H. Mathiesen, G. Zimmermann. XRMON-GF Experiments Devoted to the in Situ X-ray Radiographic Observation of Growth Process in Microgravity Conditions, Microgravity Science and Technology 26 (2014) 37-50.
[32] C. Rakete, C. Baumbach, A. Goldschmidt, D. Samberg, C.G. Schroer, F. Breede, C. Stenzel, G. Zimmermann, C. Pickmann, Y. Houltz, C. Lockowandt, O. Svenonius, P. Wiklund, R.H. Mathiesen. Compact x-ray microradiograph for in situ imaging of solidification processes: Bringing in situ x-ray micro-imaging from the synchrotron to the laboratory, Review of Scientific Instruments 82 (2011) 105108.
[33] Y. Xu, D. Casari, R.H. Mathiesen, Y. Li. Revealing the heterogeneous nucleation behavior of equiaxed grains of inoculated Al alloys during directional solidification, Acta Materialia 149 (2018) 312-325.
[34] A. Prasad, E. Liotti, S.D. McDonald, K. Nogita, H. Yasuda, P.S. Grant, D.H. StJohn. Real-time synchrotron x-ray observations of equiaxed solidification of aluminium alloys and implications for modelling, IOP Conference Series: Materials Science and Engineering 84 (2015) 012014.